



Published in final edited form as:

Trends Neurosci. 2018 December ; 41(12): 880–884. doi:10.1016/j.tins.2018.09.005.

An Inconvenient Truth: Calcium Sensors Are Calcium Buffers

Shane M. McMahon and Meyer B. Jackson

Department of Neuroscience, University of Wisconsin – Madison

Abstract

Recent advances in Ca^{2+} imaging have given neuroscientists a tool to follow the activity of large numbers of individual neurons simultaneously *in vivo* in the brains of animals as they are presented with sensory stimulation, respond to environmental challenges, and engage in behaviors. The Ca^{2+} sensors used to transduce changes in cellular Ca^{2+} into changes in fluorescence must bind Ca^{2+} to produce a signal. By binding Ca^{2+} , these sensors can act as buffers, often reducing the magnitude of a Ca^{2+} change several fold and producing a proportional slowing of the rates of change. Ca^{2+} probes can thus distort the patterns of activity they are intended to study and modify ongoing Ca^{2+} signaling functions. Recognizing these factors will enhance the use of *in vivo* Ca^{2+} imaging in the investigation of neural circuit function.

Keywords

Calcium imaging; Calcium sensors; In vivo imaging; Two-photon microscopy

The impact of Ca^{2+} probes on Ca^{2+} signals

Any molecule that binds Ca^{2+} can influence its dynamics. All fluorescent Ca^{2+} sensors currently in use, including both synthetic and genetically-encoded probes, report the presence of Ca^{2+} through a binding induced change in fluorescence. If the sensor binds to an appreciable fraction of cellular Ca^{2+} then it will act as a buffer to limit the magnitude of changes in Ca^{2+} concentration and reduce their speed. This action will depend critically on the affinity and concentration of the sensor. If a sensor's buffering is strong, it will provide a distorted picture of neuronal activity and perturb a neuron's Ca^{2+} signaling. Although the buffering actions of Ca^{2+} probes are well recognized [1–3], they are often overlooked and underestimated. In fact, the buffering action of a probe can dominate observed Ca^{2+} signals. In this Opinion we revisit some early evidence for Ca^{2+} buffering by probes, and review the well-established framework for the quantitative analysis of buffering strength. We then discuss the magnitudes of these effects and their impact on experiments, concluding with suggestions for estimating the impact of Ca^{2+} probes on Ca^{2+} imaging experiments.

Correspondence: Meyer.Jackson@Wisc.Edu.

Publisher's Disclaimer: This is a PDF file of an unedited manuscript that has been accepted for publication. As a service to our customers we are providing this early version of the manuscript. The manuscript will undergo copyediting, typesetting, and review of the resulting proof before it is published in its final citable form. Please note that during the production process errors may be discovered which could affect the content, and all legal disclaimers that apply to the journal pertain.

The buffering action of a Ca^{2+} probe is illustrated in Fig. 1 taken from an early fluorometric Ca^{2+} imaging experiment [4]. The Ca^{2+} -sensitive fluorescent dye fura-2 was loaded into a chromaffin cell through a patch pipette (Fig. 1A). The loading was monitored by observing the fluorescence elicited by 360 nm light, a wavelength that excites both Ca^{2+} -bound and free fura-2 roughly equally, so this signal does not depend on Ca^{2+} . This trace shows that the fura-2 from the patch pipette fills the cell in about 5 minutes. At the plateau in fluorescence, the concentration of fura-2 in the cell reached that in the patch pipette, 400 μM . As the loading progressed, voltage pulses of a set amplitude and duration were applied repeatedly to open Ca^{2+} channels and raise intracellular free Ca^{2+} ($[\text{Ca}^{2+}]_i$). These Ca^{2+} rises were signaled by transient reductions in fluorescence elicited by 390 nm light, a wavelength that preferentially excites the free species of fura-2. The $[\text{Ca}^{2+}]_i$ computed from the ratio of the two spectral channels illustrates two important consequences of buffering by the Ca^{2+} sensor: the voltage-induced increase in $[\text{Ca}^{2+}]_i$ declines from nearly 0.5 μM early in the loading process to about 50 nM at the plateau; and the decay time increases from a few seconds to nearly half a minute. Note that the final voltage pulse in the sequence was 500 msec instead of 50 msec to demonstrate that a large $[\text{Ca}^{2+}]_i$ transient could still be evoked but with a slow decay. This experiment demonstrates convincingly that the sensor strongly buffers intracellular Ca^{2+} . This study also reversed the buffering effect by establishing a new patch clamp recording with a lower fura-2 concentration (Fig. 1B). The $[\text{Ca}^{2+}]_i$ transients then reverted to their larger and aster character seen early in the loading process. Similar probe loading sequences were reported in septal neurons [5] and proximal dendrites of neocortical pyramidal cells [6].

Quantifying buffering actions

The buffering actions of fluorescent Ca^{2+} sensors came to light in studies of the role of Ca^{2+} in exocytosis [4] and excitation-contraction coupling [7]. This work played an essential conceptual role in elucidating how Ca^{2+} serves as a signal in these processes, and led to the development of quantitative tools for understanding the impact of buffers on Ca^{2+} fluorescent imaging. The amount of buffering by a Ca^{2+} -binding molecule, B , under a particular set of experimental conditions can be expressed as the buffering capacity, k [1, 4, 7].

$$K = \frac{\Delta[\text{CaB}]}{\Delta[\text{Ca}^{2+}]} = \frac{K_d[B]}{(K_d + [\text{Ca}^{2+}])^2} \quad (1)$$

K is the ratio of the change in bound Ca^{2+} to the change in free Ca^{2+} , and K_d is the dissociation constant of B . The binding sites of endogenous Ca^{2+} buffers saturate as Ca^{2+} rises [8–11], so k decreases as $[\text{Ca}^{2+}]$ rises. But κ provides a useful index of the impact of Ca^{2+} increments at a given ambient concentration. The experiment illustrated in Fig. 1A used a high concentration of fura-2 (400 μM) in order to demonstrate clearly the buffering action of the dye. For this concentration fura-2 contributes a κ of 889 (with $K_d = 200 \text{ nM}$ and a nominal resting $[\text{Ca}^{2+}]_i$ of 100 nM). Thus, considering only fura-2, the sensor binds 99.9% of entering Ca^{2+} at rest, leaving only about 0.1% as free ion in solution.

Many proteins and metabolites also bind Ca^{2+} , and these endogenous buffers work together with a sensor in an additive fashion to shape Ca^{2+} transients. Taking the endogenous and sensor buffering capacities as κ_e and κ_s , respectively, it can be shown that when a Ca^{2+} addition produces a change in total Ca^{2+} of $\Delta[\text{Ca}^{2+}]_{\text{Total}}$, free Ca^{2+} changes by [4]

$$\Delta[\text{Ca}^{2+}]_i = \Delta[\text{Ca}^{2+}]_{\text{Total}} / (1 + \kappa_s + \kappa_e) \quad (2)$$

The two buffers prolong the observed decay time, τ_{obs} , by the same factor

$$\tau_{\text{obs}} = \tau_0(1 + \kappa_s + \kappa_e) \quad (3)$$

where τ_0 is the decay time in the absence of any buffer. The effects of the endogenous buffers on a Ca^{2+} signal, through κ_e , are biological, while the effects of the sensor, through κ_s , are artifacts. Given this additive action of buffers, we can anticipate that a Ca^{2+} sensor will dominate Ca^{2+} dynamics as κ_s surpasses κ_e .

Implications for Ca^{2+} imaging experiments

The above reasoning indicates that one can assess the impact of the Ca^{2+} buffering action of a probe by comparing κ_s and κ_e . κ_e values have a range of roughly 50–500 [1]. A value of 100 is fairly typical, although recent work in one particular cell type gave a value of only 20 [12]. According to Eq. 1, with $[\text{Ca}^{2+}]_i = 100$ nM fura-2 will have a $\kappa_s = 20$ at a concentration of only 450 nM. Most imaging systems could not detect the fluorescence of a dye at such a low concentration. Even a more typical κ value of 100 corresponds to $[\text{fura-2}] = 2.25$ μM , which is on a Ca^{2+} signal, through κ_e , are biological, while the effects of the sensor, through κ_s , are artifacts. Given this additive action of buffers, we can anticipate that a Ca^{2+} sensor will dominate Ca^{2+} dynamics as κ_s surpasses κ_e . The above reasoning indicates that one can assess the impact of the Ca^{2+} buffering action of a probe by comparing κ_s and κ_e . κ_e values have a range of roughly 50–500 [1]. A value of 100 is fairly typical, although recent work in one particular cell type gave a value of only 20 [12]. According to Eq. 1, with $[\text{Ca}^{2+}]_i = 100$ nM fura-2 will have a $\kappa_s = 20$ at a concentration of only 450 nM. Most imaging systems could not detect the fluorescence of a dye at such a low till usually too low to use. Thus, if there is enough sensor to image Ca^{2+} , then there is almost certainly enough to produce major distortions of Ca^{2+} signals. In hippocampal axons filled with known concentrations by patch loading, extrapolating to zero sensor yielded action potential-induced Ca^{2+} rises that were 20-fold higher and decays that were 20-fold faster than those seen in fura-2-AM loaded axons [10]. In the absence of a sensor, Ca^{2+} transients decay in tens of milliseconds in spines, thin dendritic shafts [13], and nerve terminals [10]; in less than 100 msec in thick dendrites adjacent to the soma [6]; and perhaps hundreds of milliseconds in cell bodies [5, 14]. Thus, the decay times of seconds often seen in Ca^{2+} imaging experiments *in vivo* suggest that probe buffering is a dominant force. The strong buffering action of the probe in typical experiments can have serious consequences. For instance, by dominating Ca^{2+} dynamics a probe could alter the timing of responses in

sequential activations of different cells in a circuit Slowing down Ca^{2+} changes could mask timing differences and create the appearance of synchrony.

Ca^{2+} probes can also disrupt Ca^{2+} -dependent cellular signaling and thus alter cellular function. Injecting chelators into the squid giant synaptic terminal reduced release [15], so one should expect Ca^{2+} probes to have a similar action. GCaMP6m expression in the calyx of Held synaptic terminal decreased synaptic vesicle release and slowed short-term depression [16]. Transgenic mice expressing GCaMP6 had a higher incidence of epileptiform events [17], probably because lower rises in intracellular Ca^{2+} reduced the activation of Ca^{2+} -activated K^+ channels.

There has been a surge of studies using Ca^{2+} imaging to monitor electrical activity *in vivo* during behavior [e.g. 18–21]. In many of these studies, there seems to be little indication that the buffering action of the Ca^{2+} sensor is fully recognized. The Ca^{2+} sensor is introduced either by bolus injection of the AM-ester form of the dye [22], or by expression of a protein that serves as a genetically-encoded Ca^{2+} sensor [23, 24]. With both methods the cytosolic concentration of the sensor is almost impossible to control. But by the logic outlined above, if one can see its fluorescence then the sensor is almost certainly having an impact on cellular Ca^{2+} dynamics. In fact, because of the problem of tissue autofluorescence, in order to image Ca^{2+} *in vivo* the cytosolic concentration of the probe must be quite high to see over background. One might argue that the fluorescence of a Ca^{2+} sensor still reports the electrical activity during behavior, and that the distortions are only relevant to mechanistic studies of Ca^{2+} dynamics. However, differences in the signal amplitudes between cells may simply reflect different levels of probe expression. Brighter cells might appear less active because their higher sensor concentrations suppress Ca^{2+} changes. Furthermore, two cells with the same level of sensor but different k_e values would also appear different in terms of Ca^{2+} signaling because the probe would buffer a greater fraction of entering Ca^{2+} in the low- k_e cell compared to the high- k_e cell.

Concluding remarks and future perspectives

Researchers will be able to use the techniques of *in vivo* Ca^{2+} imaging more effectively if they recognize the artifacts caused by Ca^{2+} sensors. The direct determination of k_e and k_s is not practical in many kinds of experiments. Nevertheless, researchers can take some measures to address the buffering action of a Ca^{2+} sensor. Low affinity dyes are weaker buffers, but also produce smaller fractional fluorescence changes for physiological changes in Ca^{2+} . Calibration of the optical system against test samples of probe, along with assessment of tissue autofluorescence will permit probe brightness within a voxel to be converted to obtain a rough measure of probe concentration. The fluorescence of beads implanted in tissue could be compared to the fluorescence of beads in a transparent medium to assess the impact of tissue light scattering on excitation and light collection. In principle, with an estimate of sensor concentration one could use Eq. 1 to calculate K_s from the K_d and a nominal resting free $[\text{Ca}^{2+}]_i$. This can be difficult, though, because free $[\text{Ca}^{2+}]_i$ is often unknown, probe affinities differ between *in vitro* and *in vivo* environments, and the fraction of cytosolic volume accessible to the probe is not precisely known. The accumulated impact of these factors could be quite large. Another approach to evaluating the impact of a Ca^{2+}

sensor is based on decay times. The much longer decay times in virtually all the *in vivo* reports indicate that the sensor is buffering. One can estimate the decay time of an evoked Ca^{2+} rise by patch clamping a neuron with a known probe concentration. For a rapidly equilibrating dye, the extrapolation to zero dye concentration will give the biologically relevant decay time for a Ca^{2+} rise, $\tau_{\text{obs}} = \tau_0(1 + k_c)$ from Eq. 3. The prolongation of this decay time under less well defined loading conditions would then provide an indication of the impact of the sensor, including its increment to k from k_d . As *in vivo* Ca^{2+} imaging advances, attention to these issues will enhance the power of a technique that is offering unique and remarkable insights into the function of the nervous system.

Acknowledgements

We thank Dr. Chih-Tien Wang for helpful comments on the manuscript. Supported by NIH grant NS103206.

References

1. Neher E (1995) The use of fura-2 for estimating Ca buffers and Ca fluxes. *Neuropharmacology* 34, 1423–1442. [PubMed: 8606791]
2. Grienberger C and Konnerth A (2012) Imaging calcium in neurons. *Neuron* 73 (5), 862–85. [PubMed: 22405199]
3. Higley MJ and Sabatini BL (2008) Calcium signaling in dendrites and spines: practical and functional considerations. *Neuron* 59 (6), 902–13. [PubMed: 18817730]
4. Neher E and Augustine GJ (1992) Calcium gradients and buffers in bovine chromaffin cells. *Journal of Physiology* 450, 273–301. [PubMed: 1331424]
5. Schneggenburger R et al. (1993) Fractional contribution of calcium to the cation current through glutamate receptor channels. *Neuron* 11 (1), 133–43. [PubMed: 7687849]
6. Helmchen F et al. (1996) Ca^{2+} buffering and action potential-evoked Ca^{2+} signaling in dendrites of pyramidal neurons. *Biophys J* 70 (2), 1069–81. [PubMed: 8789126]
7. Berlin JR et al. (1994) Intrinsic cytosolic calcium buffering properties of single rat cardiac myocytes. *Biophys J* 67 (4), 1775–87. [PubMed: 7819510]
8. Zhou Z and Neher E (1993) Mobile and immobile calcium buffers in bovine adrenal chromaffin cells. *J Physiol* 469, 245–73. [PubMed: 8271200]
9. Xu T et al. (1997) Kinetic studies of Ca^{2+} binding and Ca^{2+} clearance in the cytosol of adrenal chromaffin cells. *Biophys J* 73 (1), 532–45. [PubMed: 9199815]
10. Jackson MB and Redman SJ (2003) Calcium dynamics, buffering, and buffer saturation in the boutons of the dentate granule-cell axons in the hippocampus. *Journal of Neuroscience* 23, 1612–1621. [PubMed: 12629165]
11. McMahon SM et al. (2016) Multiple cytosolic calcium buffers in posterior pituitary nerve terminals. *J Gen Physiol* 147 (3), 243–54. [PubMed: 26880753]
12. Lin KH et al. (2017) Dynamics of volume-averaged intracellular Ca^{2+} in a rat CNS nerve terminal during single and repetitive voltage-clamp depolarizations. *J Physiol* 595 (10), 3219–3236. [PubMed: 27957749]
13. Sabatini BL et al. (2002) The life cycle of Ca^{2+} ions in dendritic spines. *Neuron* 33 (3), 439–52. [PubMed: 11832230]
14. Tatsumi H and Katayama Y (1993) Regulation of the intracellular free calcium concentration in acutely dissociated neurons from rat nucleus basalis. *J Physiol* 464, 165–81. [PubMed: 8229797]
15. Adler EM et al. (1991) Alien intracellular calcium chelators attenuate neurotransmitter release at the squid giant synapse. *J Neurosci* 11 (6), 1496–507.
16. Singh M et al. (2018) Presynaptic GCaMP expression decreases vesicle release probability at the Calyx of Held. *Synapse*

17. Steinmetz NA et al. (2017) Aberrant Cortical Activity in Multiple GCaMP6-Expressing Transgenic Mouse Lines. *E Neuro* 4 (5).
18. Ohki K et al. (2005) Functional imaging with cellular resolution reveals precise micro-architecture in visual cortex. *Nature* 433 (7026), 597–603. [PubMed: 15660108]
19. Goncalves JT et al. (2013) Circuit level defects in the developing neocortex of Fragile X mice. *Nat Neuro sci* 16 (7), 903–9.
20. Sofroniew NJ et al. (2016) A large field of view two-photon meso scope with subcellular resolution for in vivo imaging *Elife*5.
21. Stirman JN et al. (2016) Wide field-of-view, multi-region, two-photon imaging of neuronal activity in the mammalian brain. *Nat Bio technol* 34 (8), 857–62.
22. Stosiek C et al. (2003) In vivo two-photon calcium imaging of neuronal networks. *Proc Natl A cad Sci U S A* 100 (12), 7319–24.
23. Knopfel T et al. (2010) Toward the second generation of optogenetic tools. *J Neuro sci* 30 (45), 14998–5004.
24. Akerboom J et al. (2013) Genetically encoded calcium indicators for multi-color neural activity imaging and combination with optogenetics. *Front Mol Neuro sci* 6, 2.

Outstanding Questions

- How do Ca^{2+} sensors alter the patterns of observed neural activity?
- How much do Ca^{2+} sensors alter Ca^{2+} signaling functions of a neuron during sensory input processing and the generation of behavior?
- Can technological advances mitigate the artifacts due to Ca^{2+} buffering by Ca^{2+} sensors?

Highlights

- Although the buffering actions of Ca^{2+} sensors are widely known, their magnitude and impact are often not fully appreciated. This buffering action will reduce the amplitude of a change in intracellular Ca^{2+} and prolong the decay.
- The magnitude of this buffering action is reflected in a sensor's buffering capacity, which depends on the concentration and affinity of the sensor. The buffering capacity of a sensor exceeds the buffering capacity of endogenous Ca^{2+} buffers (Ca^{2+} -binding proteins and metabolites) under the conditions that pertain during most Ca^{2+} imaging experiments. As a result, the Ca^{2+} sensor will have a dominant effect on Ca^{2+} signals.
- Recognizing the impact of the Ca^{2+} sensors used for Ca^{2+} imaging of intracellular Ca^{2+} will allow investigators to use these tools more effectively.

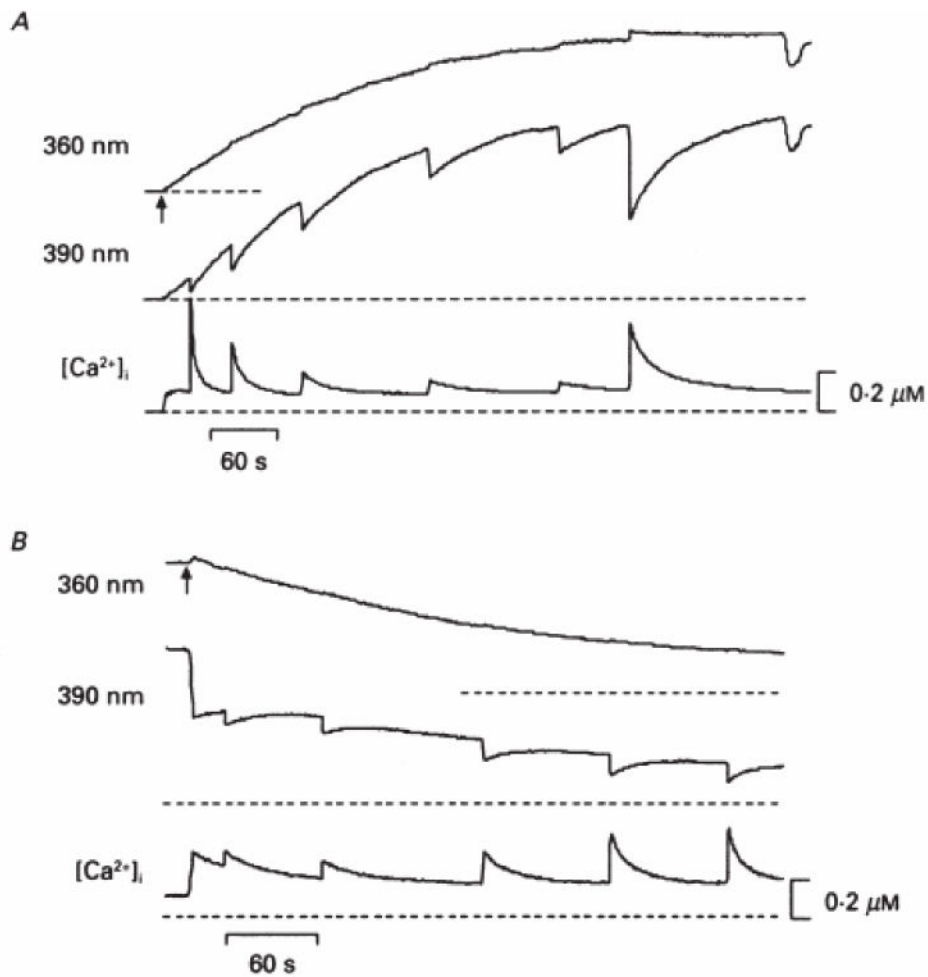


Figure 1. Ca^{2+} buffering by the Ca^{2+} sensor fura-2 in chromaffin cells.

A. In a patch clamped chromaffin cell, the fluorescence of the dye is excited with two different wavelengths nearly simultaneously by rapid switching between excitation filters. The fluorescence at the Ca^{2+} -independent wavelength (360 nm, top trace) gives the time course of fura-2 loading into the cell. Voltage pulses of 50 msec from -70 mV to 10 mV were applied at irregular intervals during the loading, and dips in the Ca^{2+} -sensitive wavelength (390 nm, middle trace) reported Ca^{2+} rises. The final fluorescence change was elicited by a longer voltage pulse of 500 msec. The intracellular free Ca^{2+} concentration, $[Ca^{2+}]_i$, computed from the ratio of fluorescence elicited by the two wavelengths (bottom trace), illustrates the decrease in amplitude of the $[Ca^{2+}]_i$ rise and increase in decay time as $[fura-2]$ in the cell rises to a final concentration of $400 \mu M$. **B.** After removing the patch electrode containing $400 \mu M$ fura-2, a second recording was made from the same cell using a patch pipette containing $50 \mu M$ fura-2. The decline in fluorescence at 360 nm tracked the reduction in fura-2 concentration. As the dye concentration fell, the Ca^{2+} rises evoked by 20 msec pulses became larger and the decays became more rapid. Extracellular Ca^{2+} was 5 mM. Reproduced with permission from Neher and Augustine, 1992 [4].